View metadata, citation and similar papers at core.ac.uk

brought to you by CORE

provided by Open Archive Toulouse Archive Ouverte

Open Archive Toulouse Archive Ouverte (OATAO)

OATAO is an open access repository that collects the work of some Toulouse researchers and makes it freely available over the web where possible.

This is an author's version published in: https://oatao.univ-toulouse.fr/22988

Official URL: https://ieeexplore.ieee.org/document/6101029

To cite this version :

Bidon, Stéphanie and Deudon, François and Krasnov, Oleg and Le Chevalier, François Coherent Integration for Wideband LFMCW Applied to PARSAX Experimental Data. (2011) In: 8th European Radar Conference (EURAD 2011), 12 October 2011 - 14 October 2011 (Manchester, United Kingdom).

Any correspondence concerning this service should be sent to the repository administrator:

tech-oatao@listes-diff.inp-toulouse.fr

Coherent Integration for Wideband LFMCW Applied to PARSAX Experimental Data

Stéphanie Bidon [#1], François Deudon [#2], Oleg A. Krasnov [†3], François Le Chevalier [†*4]

[#] *Department Electronics Optronics and Signal, University of Toulouse/ISAE, Toulouse, France*
[1] sbidon@isae.fr
[2] fdeudon@isae.fr

[†] *International Research Centre for Telecommunications and Radar, Delft University of Technology Delft, The Netherlands*
[3] O.A.Krasnov@tudelft.nl
[4] f.lechevalier@tudelft.nl

[*] *Thales Air Operations Rungis, France*

***Abstract*— In this paper, we present a coherent integration algorithm designed for the PARSAX radar system in case of wideband waveform. The technique is applied to experimental data collected on November 2010.**

I. Introduction

Non-ambiguous radar mode may be obtained with a *single* pulse repetition frequency (PRF) for radar systems having a large fractional bandwidth and a low PRF. Though very appealing, the implementation of such modes first requires several challenges to be overcome—with respect to the hardware and signal processing design [1]–[4].

The International Research Centre for Telecommunications and Radar (IRCTR) at the Delft University of Technology (TU-Delft) has been developing these last years a polarimetric agile radar in S- and X-band (PARSAX) [5]. Recently, the PARSAX radar system has been shown to work well with waveform having bandwidth up to 100MHz in S-band. A near-wideband mode is thus currently available. More specifically, measurement series have been collected on November 2010 for studying performance of wideband processing techniques.

Wideband radar signal processing has to overcome the problem of range migration that occurs for fast moving scatterers due to the high range resolution. Coherent integration techniques have been proposed in the literature in case of range-migrating targets so as to preserve the gain on the target peaks [1], [6]. *In this paper, we intend to elaborate and apply a wideband coherent integration technique to the experimental data collected from the PARSAX radar.*

The remaining of the paper is organized as follows. In section II, the measurement scenario of November 2010 is described. Then, in section III, a data model is developed in accordance with the experimental setup. Given the formalism of the model so obtained, we propose in section IV to apply a dedicated coherent integration algorithm to the trials. Conclusions are drawn in section V.

The work of F. Deudon is supported by the Délégation Générale de l'Armement (DGA) and by Thales Systèmes Aéroportés.

The PARSAX project is funded by the Dutch Technology Foundation STW.

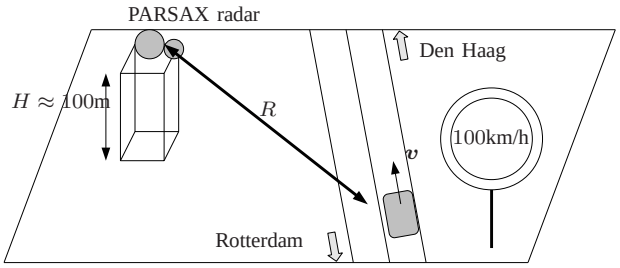

Fig. 1. Experimental setup.

II. Measurement scenario

In this section, the experimental setup as well as the waveform and the pre-processing chain of the PARSAX data are described.

A. Experimental setup

The PARSAX radar system is situated on the rooftop of the EEMCS[1] building at TU-Delft at a height of about $H \approx 100m$. Transmitter and receiver antennas are two parabolic reflectors that are isolated from one another and will be considered as co-located. For the experiment, the radar mainlobe has been pointed towards the Rotterdam/Den Haag freeway during a heavy traffic time, so that our targets of interest are non-cooperative vehicles. The steering direction is more precisely $(\phi, \theta) = (132^o, -3.2^o)$ where ϕ is the azimuth defined from a north based line and θ is the elevation. Hence, mainlobe ranges are spanning around $R \approx 1.8$km. Geometry of the scenario is represented in Fig. 1.

[1] Electrical Engineering, Mathematics, and Computer Science.

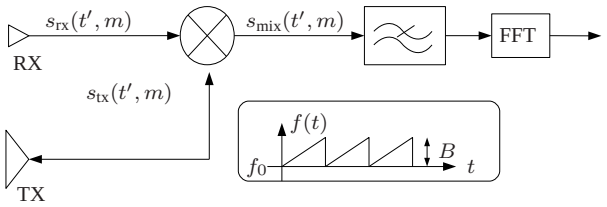

Fig. 2. Simplified scheme of the PARSAX design.

B. Waveform and data pre-processing

The PARSAX radar has a very flexible architecture regarding the generated waveform as well as the pre-processing algorithms performed in the digital receiver.

For the experiment, a linearly frequency modulated continuous waveform (LFMCW) has been chosen with an instantaneous bandwidth $B = 100$MHz. The current configuration of the radar allows one to work with an S-band carrier equal to $f_0 = 3.315$GHz. Therefore, a near-wideband mode is obtained with a fractional bandwidth equal to $B/f_0 \approx 3\%$ and a range resolution of $\delta_R \approx c/(2B) = 1.5$m. A low PRF mode has been chosen with a pulse repetition interval (PRI) equal to $T_r = 1$ms. Hence, there is no range ambiguity and the ambiguous velocity is equal to $v_a = c/(2f_0T_r) \approx 45.25$m/s ($c$ is the speed of light). Given the speed limitation and the geometry of the experiment, the maximum velocity expected for a target is about 28m/s. Hence, fast moving vehicles are aliased in velocity if one is interested in the velocity sign.

In case of LFM waveform, the PARSAX digital receiver performs the matched filtering via a deramping processing as depicted in Fig. 2. The figure represents a simplified architecture that will be sufficient to derive a data model with respect to the measurement scenario in section III. After mixing both received and transmitted signals, the low pass filter excludes echoed signal beyond $R_{\max} \approx 7.5$km when $B = 100$MHz. Note that the polarimetric capability of the PARSAX radar has not been exploited in this study. Only the HH-polarized signals have been used.

III. PARSAX SIGNAL MODEL

Herein, we derive the data model for the PARSAX signal with respect to the measurement scenario described in section II. It is shown that the formalism of the model is similar to those developed for wideband signals in [6]–[8].

A. Raw signal received from a single scatterer

The radar sends a series of M sweeps

$$s_{\text{tx}}(t) = \sum_{m=0}^{M-1} u(t - mT_r)e^{j2\pi f_0 t} \tag{1}$$

where $u(t)$ denotes the complex[2]envelope of the waveform. For LFMCW, the envelope can be expressed as

$$u(t) = e^{j2\pi\frac{\beta}{2}t^2}\,\Pi_{[0,T_r]}(t)$$

[2]For the sake of simplicity a complex de-ramping processing is assumed.

where β is the sweep rate

$$\beta = \frac{B}{T_r}.$$

If the propagating wave encounters a scatterer along its path, part of its energy is backscattered towards the radar so that the received signal can be approximated by

$$s_{\text{rx}}(t) \propto s_{\text{tx}}\left(t - \tau(t)\right)$$

where $\tau(t)$ represents the round-trip delay and $\propto$ means proportional to. If one assumes that the target has a constant radial velocity v during the coherent processing interval (CPI) and that $v \ll c$, the round-trip delay can be expressed by

$$\tau(t) = \frac{2R_0}{c} - \frac{2v}{c}t = \tau_0 - \frac{2v}{c}t \tag{2}$$

where τ_0 and R_0 are the initial delay and range of the scatterer. Plugging (2) in (1), one obtains

$$\begin{aligned} s_{\text{rx}}(t) \propto \sum_{m=0}^{M-1} & e^{j\pi\beta\left[\left(1+\frac{2v}{c}\right)t-\tau_0-mT_r\right]^2}\Pi_{[0,T_r]}(t - mT_r - \tau_0) \\ & \times e^{j2\pi f_0\left(1+\frac{2v}{c}\right)t} \end{aligned} \tag{3}$$

where we have assumed that the Doppler effect is negligible on the M gates function $\Pi_{[0,T_r]}$, i.e., $2|v|/c \ll 1 + 2v/c$. By introducing the fast-time $t' = t - mT_r$, the mth received sweep is given by

$$\begin{aligned} s_{\text{rx}}(t', m) \propto & e^{j\pi\beta\left[\left(1+\frac{2v}{c}\right)t'-\tau_0+\frac{2v}{c}mT_r\right]^2}e^{j2\pi f_0\left(1+\frac{2v}{c}\right)(t'+mT_r)} \\ & \times\Pi_{[0,T_r]}(t' - \tau_0). \end{aligned} \tag{4}$$

Note that the phase rotation due to the Doppler in the first term of (4) is negligible, i.e., $2\pi B(2v/c)T_r \ll 1$ or equivalently

$$vT_r \ll \frac{c}{2B} \tag{5}$$

which leads to

$$\begin{aligned} s_{\text{rx}}(t', m) \propto & e^{j\pi\beta\left[t'-\tau_0+\frac{2v}{c}mT_r\right]^2}e^{j2\pi f_0\left(1+\frac{2v}{c}\right)(t'+mT_r)} \\ & \times\Pi_{[0,T_r]}(t' - \tau_0). \end{aligned} \tag{6}$$

B. Deramping

The (range) matched filtering is performed via a deramping processing where both received and transmitted signal are mixed, low-pass filtered and then transformed in the "beat-frequency" domain via a fast Fourier transform (FFT).

1) Mixing RX/TX: The mth received sweep (6) is multiplied with the complex conjugate of the mth transmitted sweep given by

$$s_{\text{tx}}(t', m) \propto e^{j\pi\beta t'^2}e^{j2\pi f_0(t'+mT_r)}\Pi_{[0,T_r]}(t'). \tag{7}$$

The mixing operation is limited to the time interval $[\tau_{\max}, T_r]$ where $\tau_{\max}$ is the round-trip delay of a target located at the maximum observed range, i.e., $\tau_{\max} = 2R_{\max}/c$. The mixed signal is thus given by

$$\begin{aligned} s_{\text{mix}}(t', m) \propto & e^{j\pi\beta\left\{2\left(-\tau_0+\frac{2v}{c}mT_r\right)t'+\left[\tau_0^2+\left(\frac{2v}{c}mT_r\right)^2-2\tau_0\frac{2v}{c}mT_r\right]\right\}} \\ & \times e^{j2\pi f_0\frac{2v}{c}(t'+mT_r)}\Pi_{[\tau_{\max},T_r]}(t'). \end{aligned} \tag{8}$$

Note that in (8), quadratic terms are either constant or negligible (indeed, $B\left(\frac{2v}{c}MT_r\right)^2 \ll 1$) , so that the mixed signal can be approximated by

$$s_{\text{mix}}(t',m) \propto e^{j2\pi\left\{\left[f_b+\beta\frac{2v}{c}mT_r\right]t'+\left[f_D-\beta\tau_0\frac{2v}{c}\right]mT_r\right\}} \times\Pi_{[\tau_{\max},T_r]}(t') \quad (9)$$

where we have recognized both the conventional Doppler frequency and the beat-frequency defined respectively by

$$f_D = f_0\frac{2v}{c} \quad (10a)$$

$$f_b = f_D - \beta\tau_0. \quad (10b)$$

At this point, three remarks are in order. First, given the expected velocities and ranges of interest, we have $|f_D| \ll \beta\tau_0$, so that the beat-frequency (11) is directly related to the initial range of the target by

$$f_b \approx -\beta\tau_0. \quad (11)$$

Secondly, note that in (9) the conventional beat-frequency f_b is affected at each sweep by the term $\beta(2v/c)mT_r$ which cannot be neglected as the following inequality

$$vMT_r > \frac{c}{2B} \quad (12)$$

holds for fast moving targets. In other words, fast moving targets migrate from one range gate to another during the CPI. Finally, note that for a given velocity, the range of expected delay ensures that

$$|f_D| = f_0\frac{2|v|}{c} \gg \beta\tau_0\frac{2|v|}{c}. \quad (13)$$

Using both (11) and (13), the mixed signal for the mth sweep can be re-written as

$$s_{\text{mix}}(t',m) \propto e^{j2\pi\left\{\left[f_b+\beta\frac{2v}{c}mT_r\right]t'+f_DmT_r\right\}}\Pi_{[\tau_{\max},T_r]}(t') \quad (14)$$

where f_b does not depend on the target velocity.

2) Low pass filtering: At this point the mixed signal (14) is low pass filtered, so that targets with range (i.e., equivalently beat-frequency) greater than $R_{\max}$ are removed from the data. In the PARSAX architecture, this operation allows one to decrease the sampling rate to $f_s = (400/22)$MHz. The digital series to be processed is thus

$$\{s_{\text{mix}}(k/f_s,m)\}_{k=0}^{K-1} \quad (15)$$

where K is the total number of samples per sweep[3], i.e., $K \approx (T_r - \tau_{\max})f_s$.

3) FFT: An FFT transform is then applied to (15) with $K_{\text{fft}} \approx 16$K points, so that the signal delivered by the current hardware in the beat-frequency/slow-time domain is given with a good approximation, for $k = 0,\ldots,K_{\text{fft}}-1$, by

$$S_{\text{mix}}(k,m) \propto e^{j2\pi f_DmT_r}\,\delta\left\{k - \frac{K_{\text{fft}}}{f_s}\left[f_b + B\frac{2v}{c}m\right]\right\} \quad (16)$$

where $\delta\{\}$ is the discrete Dirac function.

[3]The exact range resolution is given by $\delta_R = [1-\tau_{\max}/T_r]^{-1}c/(2B) \approx 1.58$m.

C. Wideband pre-processing

To obtain an adequate formalism as in [6]–[8], we propose to go further with the pre-processing operations by selecting a low range resolution segment of length $L \ll K$ that contains the target of interest and then apply a frequency-beat transform via an IFFT. Indeed, from (16), it appears that the target is mainly present on the beat-frequency interval $\{f_b,\ldots,f_b + B(2v/c)(M-1)\}$ (for $v > 0$). Without loss of generality, the target is assumed to be present in the L first beat-frequency bins $\ell = 0,...,L-1$. Hence, applying an IFFT to the L-length segment one obtains

$$S_{\text{mf}}(\ell,m) \propto e^{j2\pi f_DT_rm}e^{j2\pi\left[f_b+B\frac{2v}{c}m\right]\frac{K_{\text{fft}}}{f_s}\frac{\ell}{L}} \quad (17)$$

where $\ell = 0,\ldots,L-1$ is the beat-time index. Finally, the signature of a single scatterer in the beat-time/slow-time domain can be summed up in a matrix $\boldsymbol{A}$ whose (ℓ,m)th element is given by

$$\boxed{[\boldsymbol{A}]_{\ell,m} = e^{j2\pi\bar{f}_r\ell}e^{j2\pi\bar{f}_Dm}e^{j2\pi\mu\bar{f}_D\ell m}} \quad (18)$$

for $\ell = 0,\ldots,L-1$ and $m = 0,\ldots,M-1$ and where

$$\boxed{\bar{f}_r = -\frac{K_{\text{fft}}}{f_s}\frac{1}{T_r}\frac{\ell_0}{L}} \quad \boxed{\bar{f}_D = -f_0\frac{2v}{c}T_r} \quad (19)$$

with $\ell_0 = B\tau_0$ the initial range gate and

$$\boxed{\mu = \frac{K_{\text{fft}}}{f_s}\frac{1}{T_r}\frac{B/L}{f_0}}. \quad (20)$$

Thus, we recognize the same wideband data model as in [6], [8] up to the factor $(K_{\text{fft}}/f_s)/T_r \approx 0.9$. Note that according to (18), the observed range migration of a scatterer during the CPI is equal to $vM(K_{\text{fft}}/f_s)$. Therefore, the observed range migration for a deramped LFMCW is slightly reduced compared to the one of a pulsed waveform for which the range migration is equal to vMT_r [8].

IV. Experimental results

Given the formalism of the point-target signature (18), we define and apply herein a coherent integration associated to (18) to the PARSAX data. Due to space limitation, results are presented for one data set only. The length of the low range resolution segment is set to $L = 64$. To ensure the assumption of constant velocity and preserve coherence of the target amplitude, we process no more than $M = 128$ sweeps.

First, so as to obtain a reference point, conventional Doppler processing is applied to the data set, i.e, for $\ell = 0,\ldots,L-1$ and for $f_D \in [-0.5, 0.5[$, we derive via the FFT algorithm

$$\mathcal{D}(\ell,\bar{f}_D) = \sum_m S_{\text{mix}}(\ell,m)e^{-j2\pi\bar{f}_Dm}. \quad (21)$$

Secondly, we perform a coherent integration on (17) that compensates also the cross-coupling terms $\exp\{j2\pi\mu\bar{f}_D\ell m\}$ in (18) that accounts for the range migration. A rapid algorithm is used [9] while taking into account the modified value of the

parameter μ defined in (20) in case of deramping processing. Hence, we derive

$$S(\bar{f}_r, \bar{f}_D) = \sum_{\ell,m} S_{\text{mf}}(\ell, m)\, e^{-j2\pi\left[\bar{f}_r \ell + \bar{f}_D m + \mu \bar{f}_D \ell m\right]} \quad (22)$$

for $\ell = 0, \ldots, L-1$ and for $\bar{f}_D \in [-n_{va}/2, n_{va}/2[$ where n_{va} stands for the desired unfolding factor (here $n_{va} = 4$).

Given the results shown in Fig. 3, the following remarks are in order.

- Clutter and target returns have a high amplitude compared to the thermal noise level.
- Aliased target peaks of a conventional Doppler processing (21) are transformed into sidelobes for the coherent integration (22).
  - ◇ This allows one to alleviate partially the ambiguous velocities. Hence, from the coherent integration (22), we can infer the non-ambiguous velocity for exo-clutter targets: e.g, on Fig. 3(b), two moving vehicles have been highlighted, one has a velocity of $v_1 \approx -14$m/s, while the other has a velocity of $v_2 \approx -27\text{m/s} < (v_a/2)$.
  - ◇ However, sidelobes from the coherent integration (22) remain high. This may prevent detection in a dense-target scenario. Also, the problem of blind velocities remain especially since clutter sidelobes from each range gate tend to add up.

V. Conclusion

We have shown that the PARSAX data obtained with a bandwidth of 100 MHz have, from a theoretical point of view, the formalism of wideband data where the phenomenon of range-walk may occur. Then, a coherent integration algorithm associated to this model has been described, and the specificities of FMCW deramping, compared to pulse waveforms, has been emphasized. By applying it to experimental data, we have shown that the range migration allows one to alleviate the velocity ambiguity in a low PRF mode at least for fast exo-clutter targets. Future work may involve upgrading of the PARSAX hardware so as to obtain higher bandwidth thereby increasing the range-walk, i.e., the discrimination between clutter and moving targets.

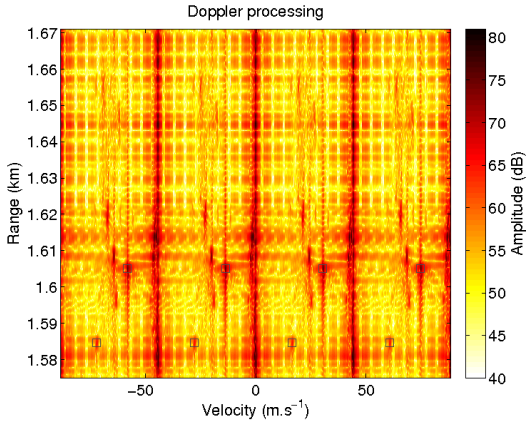

(a)

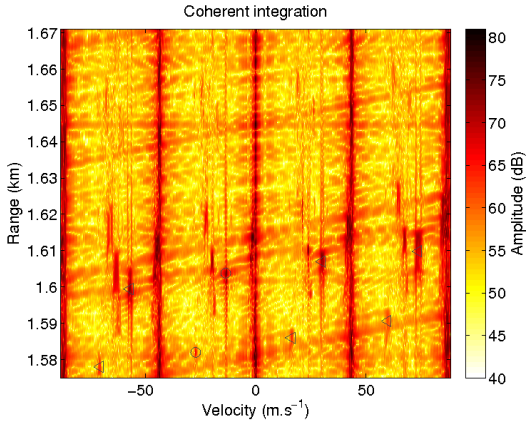

(b)

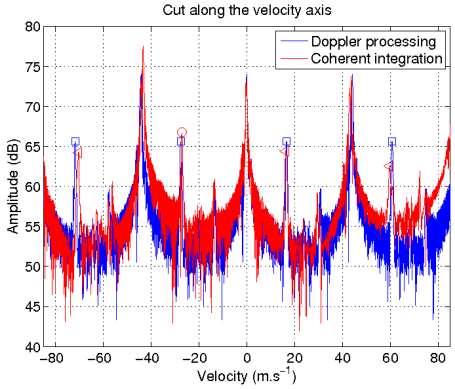

(c)

Fig. 3. Range-velocity maps: (a) Doppler processing. (b) Coherent integration. (c) Cut along the line of migration of the fast-moving target. (○ mainlobe, ◁ sidelobe , □ (aliased)-mainlobe)

References

[1] D. E. Iverson, "Coherent processing of ultra-wideband radar signals," *Proc. IEE Radar, Sonar Navig.*, vol. 141, no. 3, pp. 171–179, June 1994.

[2] A. Farina and F. A. Studer, "Detection with high resolution radar: great promise, big challenge," *Microwave J.*, vol. 34, no. 5, pp. 223–273, May 1991.

[3] M. Skolnik, "Ultrawideband microwave-radar conceptual design," *IEEE Aerosp. Electron. Syst. Mag*, May 1995.

[4] A. Becker and F. Le Chevalier, "Wideband coherent airborne radar systems: performances for moving target detection," in *Proc. Int. Conf. Radar*, 2001, pp. 146–149.

[5] O. A. Krasnov, G. P. Babur, L. P. Litghart, and F. van der Zwan, "Basics and first experiments demonstrating isolation improvements in the agile polarimetric FM-CW radar - PARSAX," in *Proc. 6th European Radar Conf.*, Rome, Italy, 30 Sep.–2 Oct. 2009, pp. 13–16.

[6] F. Le Chevalier, *Principles of Radar and Sonar signal processing*. Norwood, MA: Artech House, 2002.

[7] N. Jiang, R. Wu, and J. Li, "Super resolution feature extraction of moving targets," *IEEE Trans. Aerosp. Electron. Syst.*, vol. 37, no. 3, pp. 781–793, July 2001.

[8] F. Deudon, S. Bidon, O. Besson, J.-Y. Tourneret, M. Montécot, and F. Le Chevalier, "Modified Capon and APES for spectral estimation of range migrating targets in wideband radar," in *Proc. IEEE Int. Radar Conf.*, May 10–14, 2010.

[9] S. Bidon, L. Savy, and F. Deudon, "Fast coherent integration for migrating targets with velocity ambiguity," in *IEEE Radar Conf. 2011*, Kansas City, Missouri, May 23–27, accepted.